SAR Calculation Using Numerical Human Model Exposed to EM Wave from Commercial Wireless Terminal at 150 MHz

Shimpei Akimoto[1], Satoru Kikuchi, Kazuyuki Saito, Masaharu Takahashi, Koichi Ito

Chiba University
1-33 Yayoi-cho, Inage-ku, Chiba 263-8522, Japan
[1]s.akimoto@graduate.chiba-u.jp

***Abstract*— The commercial wireless terminal is usually hold in the vicinity of a human body, it is needed an attention for the specific absorption rate (SAR) in an abdomen. In addition, the electromagnetic (EM) waves from the wireless terminal penetrate a deep region of body, because the wavelength of the EM waves of the wireless terminal operating in VHF band is longer than those of a cellular phone operating in the GHz band. In this paper, to evaluate the SARs of a male and a female when they are wearing a wireless terminal on their abdomens, we calculated the SAR in the abdomen using the numerical human model exposed to EM waves from several positions of a normal mode helical antenna (NHA) with a metallic case.**

Key words: commercial wireless terminal, NHA, SAR, numerical human model

I. Introduction

The radio frequency (RF) devices which are usually used in the vicinity of a human body have been increasing. Therefore, it is necessary to evaluate the interaction between the electromagnetic (EM) wave and the human, because it might be expected that human body is exposed to the EM waves radiated from the RF devices. Here, the influence of the EM waves on the human body is dependent on the frequency [1]. The EM waves mainly contribute the heat effect, which is generated by the absorption of the energy, above 100 kHz. The specific absorption rate (SAR) has been usually used for the primary dosimetric parameter of the EM waves exposure in the standards [2].

$$\mathrm{SAR} = \frac{\sigma E^2}{\rho} \quad \text{[W/kg]} \qquad (1)$$

Where, σ is the conductivity of the tissue [S/m], ρ is the density of the tissue [kg/m^3], and E is the electric-field strength (r. m. s.) inside the tissue [V/m].

The SAR in the human body affected by EM wave from the cellular phones has been widely investigated [3], because the cellular phones are used in the vicinity of the human head. However, the SAR of using the commercial wireless terminal has not been investigated so much. The EM waves of these devices penetrate to the deep region of the human body because the wavelength of the EM waves of the device operating in VHF band are longer than those of a cellular phone operating in the GHz band. Therefore, it is necessary to evaluate the SAR of the human body, when they are wearing a wireless terminal on their abdomen.

In previous studies [4], [5], the SAR of human body has been calculated by replacing the NHA with a half-wavelength dipole antenna, because it is difficult to model the NHA, of which configuration is complicated. In this case, the calculated SAR is multiplied by coefficient, which is induced by the magnetic field of human surface, for the correct SAR values. In addition, the studies have been investigated on the SAR calculation by use of the homogeneous phantom of elliptic cylinder shape. However, the actual human body is heterogeneity and complicated shapes. Therefore, it is important to calculate the SAR by use of the actual wireless terminal and the high-resolution human model.

The purpose of in this study is a detailed evaluation of SAR in the human body when wearing the wireless terminal. In previous studies, the SAR in the human body by use of the male model has been widely investigated. However, the SAR of using the female model has not been investigated so much. Therefore, the SAR in the human body is calculated using realistic high-resolution whole-body models of Japanese male and female [6] exposed to EM wave from the NHA with metallic case.

II. NHA Modeling

A. Analytical model

At the beginning step, in order to evaluate the SAR of the human body when wearing a wireless terminal, the NHA with metallic case was modeled. In addition, the SAR distributions due to the calculation of a NHA with metallic case in the vicinity of the tissue-equivalent phantom were compared with the measurement for modeling's validation of NHA.

Figure 1 shows the NHA with metallic case at 150 MHz used for these calculations. It is composed of the NHA for amateur radio (D90-1018-35, by Kenwood Corporation, Tokyo, Japan) and the metallic case which simulates the amateur radio terminal. Figure 2 shows the analytical model. The distance between the antenna and surface of the phantom is 40.0 mm. The observation planes are at the surface of phantom (plane-A) and horizontal plane of the phantom including the feeding point (plane-B). In addition, the observation lines are the line passing through the coordinate origin on parallel to the x axis (line-A) and directly under the feeding point along the y axis on the horizontal plane (line-B). Here, the coordinate origin is center of surface on the phantom. The

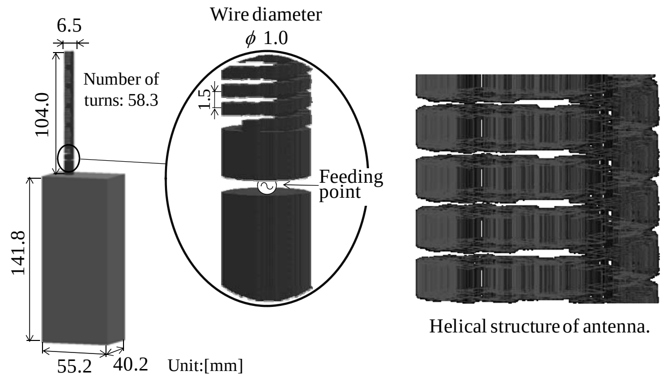

Fig. 1 NHA with metallic case.

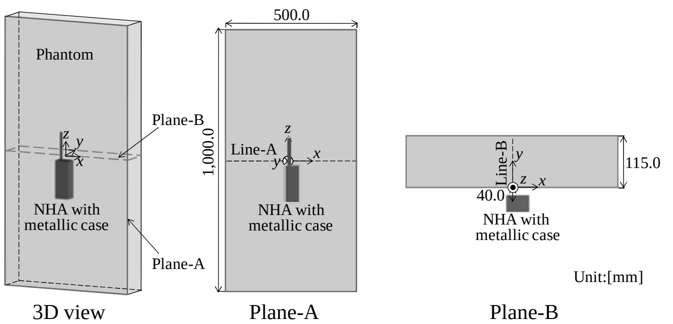

Fig. 2 Analytical model.

physical properties of the phantom are as follows: relative permittivity ε_r is 50.81; conductivity σ is 0.76 S/m; density ρ is 1,030 kg/m^3.

B. Numerical calculation

In the numerical calculation, the electric fields (*E*-field) around the antenna are calculated by the finite difference time domain (FDTD) method. This technique is a well-known effective method for the calculation of the SAR as one of the EM analyses. The parameters of FDTD calculation employed in the abdomen in this study were as follows. The cell size of NHA was 0.1 mm, and the phantom to free space was 0.1–2.0 mm. In addition, the helical structure of antenna was precisely modeled using 0.1-mm voxels (Fig. 1). Here, the coaxial cable used in the measurement was modeled as perfect electric conductor. The absorbing boundary condition was the perfectly matched layer (PML) (eight layers). Here, the calculations were performed by own FDTD code.

C. SAR measurement

Figure 3 shows the SAR measurement system. The phantom is a flat phantom filled by the tissue-equivalent liquid. In this study, the SAR distribution is measured using the DASY4 system (ver. 4.7, by Schmid & Partner Engineering AG, Zurich, Switzerland). This system is using the *E*-field probe method [7]. In this method, the SAR is evaluated by the measurement of the *E*-field distribution inside the flat phantom, which is composed by a tissue-equivalent liquid and a shell, using the isotropic *E*-field probe. This method is generally

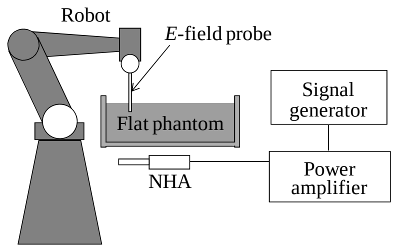

Fig. 3 SAR measurement system.

TABLE I
SAR MEASUREMENT SYSTEM

Device	Model number	Manufacturer
Signal generator	SMIQ03B	Rohde & Schwarz
Power amplifier	100W1000B	AR
Robot	RX90L	Stäubli
E-field plobe	ET3DV6	Schmid & Partner Engineering AG

used for the SAR estimation in the standards [8]. In addition, Table I shows the specification of SAR measurement system.

D. Comparison of results

Figures 4 (a) and (b) shows the calculated and the measured results of SAR distribution in the observation planes (plane-A and plane-B). Here, the radiated powers of the antennas are normalized to 1.0 W in both cases. In addition, the SAR distributions of plane-A and plane-B are 4.0 mm from the phantom surface because of the limitation of measurement area of *E*-field probe. As shown in Figs. 4 (a) and (b), the SARs at the vicinity of the antenna feeding point are highest value at both calculated and measured results. In addition, the calculated and measured SARs are distributed at $z \leq 0$ (position of metallic case). This is attributed to the effect of a coaxial cable.

Figures 5 (a) and (b) shows the SAR distributions on the observation line-A and line-B. As shown in Fig. 5 (a), the SAR of calculated result has similar tendency to the measured result on the surface of phantom. As shown in Fig. 5 (b), two results show similar tendency in deep portion of the phantom. The difference between the calculated and the measured result is within 5%. From these results, it has been observed that the measured SAR distributions agree well with calculated results.

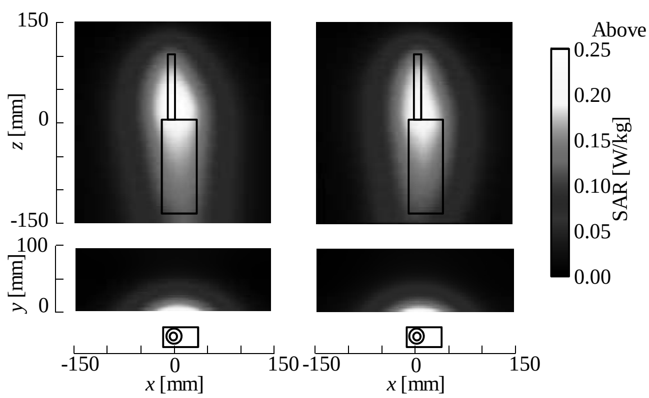

(a) Calculated result. (b) Measured result.
Fig. 4 SAR distributions in the observation planes.

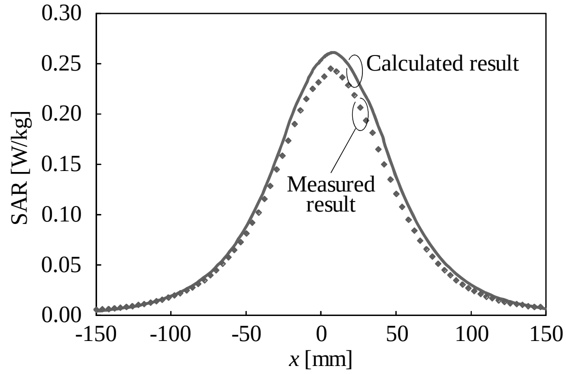

(a) Line- A.

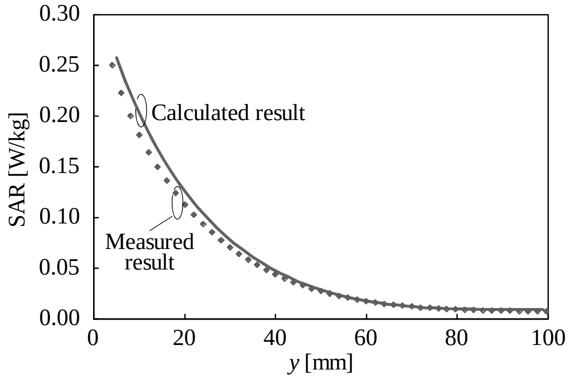

(b) Line-B.

Fig. 5 SAR distribution on observation line.

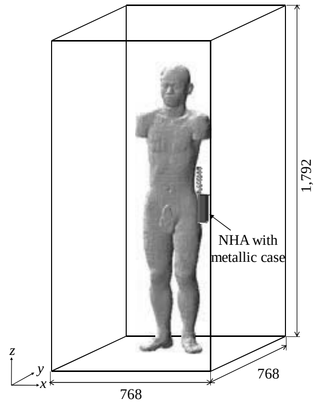

(a) Male.

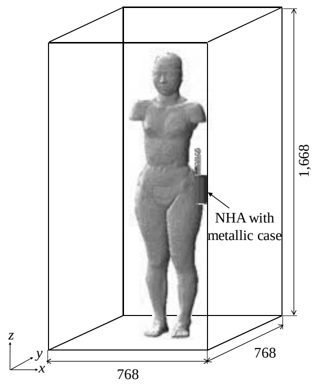

(b) Female.

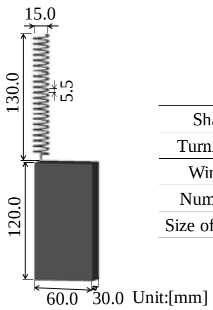

Shaft Length	130.0 mm
Turning diameter	15.0 mm
Wire diameter	1.0 mm
Number of turns	22.2
Size of metallic case	30.0 × 60.0 × 130.0 mm

(c) NHA with metallic case.

Fig. 6 Calculation model.

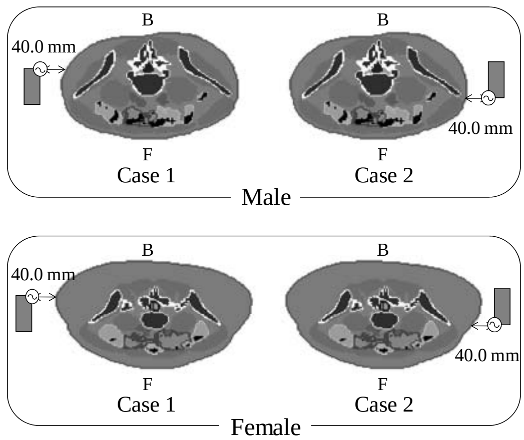

Fig.7 Horizontal planes of including the antenna feeding point.

III. SAR Calculation Using Numerical Human Model

A. Calculation model

The validity of NHA modeling is proved when the measured SAR distributions agree well with calculated results. As the following step, the SAR of human body is calculated using numerical human models (male and female) exposed to EM wave from NHA with metallic case of two positions which is as follows:

- Case 1 is in the right side of the model's waist.
- Case 2 is in the left side of the model's waist.

Figure 6 shows the calculation model. Here, Figs. 6 (a) and (b) are of case 2 as an example. In addition, the NHA was reshaped to simplify the calculation (Fig. 6 (c)). The helical structure of antenna was modeled using 0.5 mm voxels. The human models to free space were 0.5–2.0 mm. calculated regions of male and female are 768 × 768 × 1,792 mm and 768 × 768 × 1,668 mm. Figure 7 shows the horizontal planes of male and female of including the antenna feeding point. Positions of each feeding point are the same model's lumber height in view of the wearing position of folder and belt. Distances between antenna and the surface of each model were kept at 40.0 mm in order to represent a realistic situation. In addition, for convenience of calculation, the model's arms were cut off. Physical properties of the human models at 150 MHz are referred to [9], [10].

B. Calculated result

The calculated SAR results are normalized by 1.0 W radiated power from the antenna. Figures 8 (a) and (b) shows the calculated SAR distribution in the horizontal planes of male and female of including the antenna feeding point. As shown in Fig. 8, the SAR of male model is widely distributed high value (approximately 1.0 W/kg) in the deep region of the abdomen compared with that of female model. As for the causes of this, a male has a lot of muscles, whose conductivity is higher than the fat, in close to body surface compared with a female. From this result, it has confirmed that SAR distribution in the deep region of the abdomen shows different tendency by thickness of the fat under the skin and location of muscles.

Figures 9 (a) and (b) shows the 10 g averaged spatial peak SARs of male and female. Here, the 10 g averaged spatial peak SAR is calculated using the averaging technique of [11]. As shown in Fig. 9 (a), the value of case 2 is higher than case 1. One of this reason, the distance between the antenna's element and the body surface of case 2 is shorter than case 1, due to the abdomen shape. In addition, a spatial peak SAR value of male model is indicated at the body surface. In contrary, female model is indicated in muscles proximity to the antenna. The reason is according to the fact that the antenna's element is not close to the human surface for the female model.

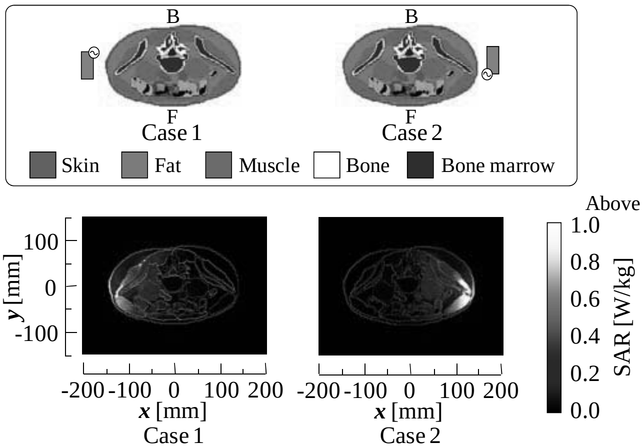

(a) Male.

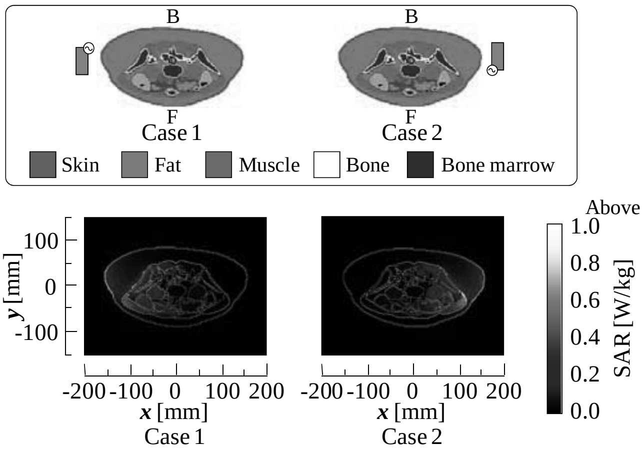

(b) Female.

Fig. 8 Calculated SAR distributions in horizontal plane.

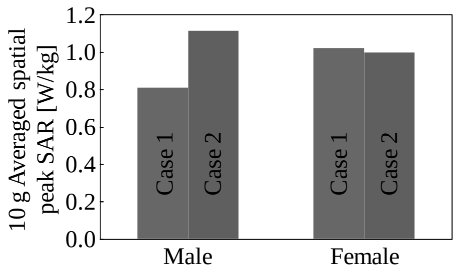

Fig. 9 10 g averaged spatial peak SAR.

IV. Conclusion

In this paper, the SAR in the human body is calculated using realistic high-resolution whole-body models of Japanese male and female exposed to EM wave from the NHA with metallic case. As a result, it has confirmed that spatial peak SARs of male and female are lower than the guidelines value (10 W/kg) under the control environment in Japan when the radiated power of the antenna is 5 W (prevalent input power of the wireless radio terminals in Japan).

Acknowledgments

The authors would like to thank Kenichi Sato, NTT Advanced Technology Corporation, Tokyo, Japan for his cooperation towards the measurement. In addition, the authors would like to thank Ryotaro Suga, Faculty of Engineering, Chiba University, Chiba, Japan for his cooperation towards the modeling of NHA. Finally, the authors would like to thank Dr. Soichi Watanabe and Dr. Lira Hamada, National Institute of Information and Communications Technology, Tokyo, Japan for their advice concerning this study.

References

[1] M. Saito, and M. Taki, "Biological effects of electromagnetic fields and health risks," J. IEICE, vol. 82, no. 6, pp. 572-579, June 1999 (in Japanese).

[2] Safety levels with respect to human exposure to radio frequency electromagnetic fields, 3 kHz to 300 GHz, ANSI/IEEE Standard C95.1-2005, Oct. 2005.

[3] A. D. Tinniswood, C. M. Furse, and O. P. Gandhi, "Computations of SAR distributions for two anatomically based models of the human head using CAD files of commercial telephones and the parallelized FDTD code," IEEE Trans. Antenna Propagat., vol. 46, no. 6, pp. 829-833, June 1998.

[4] Y. Koyanagi, H. Kawai, K. Ogawa, and K. Ito, "Consideration of the local SAR and radiation cylindroid whole body phantom at 150 MHz," IEICE Trans. Commun., vol. J85-B, no. 5, pp. 664-675, May 2002 (in Japanese).

[5] Y. Koyanagi, H. Kawai, K. Ogawa, and K. Ito, "Estimation of the local SAR in the human abdomen using a human body phantom and small antennas at 150 MHz," IEICE Trans. Commun., vol. J86-B, no. 7, pp. 1207-1218, July 2003 (in Japanese).

[6] T. Nagaoka, S. Watanabe, K. Sakurai, E. Kunieda, S. Watanabe, M. Taki, and Y. Yamanaka, "Development of realistic high-resolution whole-body voxel models of Japanese adult male and female of average height and weight and application of models to radio-frequency electromagnetic-field dosimetry," Phys. Med. Biol., Vol.49, pp.1-15, Jan. 2004

[7] N. Kuster and Q. Balzano, "Energy absorption mechanism by biological bodies in the near field of dipole antenna above 300 MHz," IEEE Trans. Veh. Tech., vol. 41, no. 1, pp. 17-23, Feb. 1992.

[8] IEC 62209-1 Human exposure to radio frequency fields from hand-held and body-mounted wireless communication devices Human models, instrumentation, and procedures Part 1: Procedure to determine the specific absorption rate (SAR) for hand-held devices used in close proximity to the ear (frequency range of 300 MHz to 3 GHz), Feb. 2004.

[9] C. Gabriel, "Compilation of the dielectric properties of body tissues at RF microwave frequencies," Brooks Air Force Technical Report AL/OE-TR-1996-0037, 1996.

[10] F. A. Duck, Physical properties of tissue: a comprehensive reference book, London, Academic Press, 1990.

[11] "IEEE Recommended practice for measurements and computations of radio frequency electromagnetic fields with respect to human exposure to such fields, 100 kHz-300 GHz," IEEE Standard C95.3-2002, 2003.